Journal of Photochemistry and Photobiology A: Chemistry 210 (2010) 181–187

Contents lists available at ScienceDirect

Journal of Photochemistry and Photobiology A: Chemistry

journal homepage: www.elsevier.com/locate/jphotochem

Transparent visible light activated C–N–F-codoped TiO_2 films for self-cleaning applications

Qing-chi Xu [a], Diana V. Wellia [a], Mahasin Alam Sk [a], Kok Hwa Lim [a], Joachim Say Chye Loo [b], Dai Wei Liao [c], Rose Amal [d], Timothy Thatt Yang Tan [a,*]

[a] School of Chemical and Biomedical Engineering, Nanyang Technological University, 62 Nanyang Drive, 637459 Singapore, Singapore
[b] School of Materials Science and Engineering, Nanyang Technological University, 50 Nanyang Avenue, Singapore 639798, Singapore
[c] Department of Chemistry, College of Chemistry and Chemical Engineering, Xiamen University, Xiamen 361005, People's Republic of China
[d] School of Chemical Sciences and Engineering, The University of New South Wales, Sydney, NSW 2052, Australia

ARTICLE INFO

Article history:
Received 4 August 2009
Received in revised form 3 December 2009
Accepted 19 December 2009
Available online 29 December 2009

Keywords:
Self-cleaning
TiO_2
Visible light
Carbon
Nitrogen
Fluorine

ABSTRACT

The current work reports a potential technology for fabricating visible light activated doped TiO_2 coatings for self-cleaning applications. Transparent C–N–F-codoped TiO_2 films with enhanced visible light photocatalytic activity and non-light activated superwettability were successfully prepared by a simple layer-by-layer dip-coating method using TiO_2 sol and NH_4F methanol solution as precursors. The current coating method prevents the reactions of F^- ions with the glass substrate and hence resulting in a uniform and transparent coating. It also creates TiO_2 coating with high surface roughness without an additional pore-inducing agent and generates non-irradiated superhydrophilic surface. Contact angles of the C–N–F-codoped TiO_2 films were 2.3–3.1° in the absence of any illumination and they rose slowly in the dark (<1.8° in 30 days). The C–N–F-codoped TiO_2 films showed strong visible-light absorption and enhanced photocatalytic activity for stearic acid decomposition under visible light irradiation, which was 5 times higher than that of C-doped TiO_2 film. Our DFT calculations also showed that increasing N:F doping ratio leads to band gap narrowing of TiO_2.

1. Introduction

TiO_2 films can potentially convert hydrophilic surface to superhydrophilic surface under UV illumination [1]. Together with its photocatalytic property, TiO_2 films have a high potential for self-cleaning and solar cell applications. UV light illumination is required to convert conventional TiO_2 film to a superhydrophilic surface and simultaneously activate the film to degrade contaminants, which limits its applications. TiO_2 nanoparticles doped with nonmetal elements (N, C, F, S, etc.) [2–5] and metal elements (Cr, V, Fe, etc.) [6–8] were widely investigated with an aim to improve the photocatalytic activity under visible light. The visible light induced super-hydrophilicity on TiO_2 films doped with nonmetal or metal elements were also reported by some groups [9–11]. Unfortunately, the photocatalytic activity of most of the doped TiO_2 was lower than that of pure TiO_2 due to the higher recombination rate of the charge carriers in the doped TiO_2 [12]. Recently, codoped TiO_2 were developed to improve the photocatalytic activity of TiO_2 under both UV and visible light. S–N-codoped TiO_2 [13], F–N-codoped TiO_2 [14], B–N-codoped TiO_2 [15] and C–N-codoped TiO_2 powder [16] were prepared to improve the photocatalytic efficiency under visible light and prevent the reduction of photocatalytic activity due to charge recombination. F–N-codoped TiO_2 powder showed higher photocatalytic activity than that of pure TiO_2, N-doped TiO_2 and F-doped TiO_2 [15,17]. Valentin and co-workers inferred that N–F codoping reduced the energy cost of doping and the amount of defects in the lattice as a consequence of the charge compensation between p-type N and n-type F impurities [17]. Both sol–gel [4] and spray pyrolysis [14] techniques had been employed to prepare N–F-codoped TiO_2 powder. Reactive DC magnetron sputtering was used to prepare N-doped TiO_2 film for solar cell application [18].

To the best of our knowledge, N–F-codoped TiO_2 films for self-cleaning applications have not been reported, possibly impeded by the fact that the F^- ions could react with glass substrates and hence making it difficult to prepare transparent N–F-codoped TiO_2 film. Another issue is the uneven coating that arises from the low dispersity of the powder and the formation of precipitation in the coating solution, which causes low transparency of the coated film. Moreover, TiO_2 or doped TiO_2 film tend to lose its superhydrophilic performance without illumination. Herein, from a practical point of view, it is desirable that the contact angles of TiO_2 films remain low or rise very slowly in the dark. It is well known that the wettability of solid surfaces is dependent on both chemical properties and geometry of solid surfaces. Superhydrophilic properties can

* Corresponding author. Tel.: +65 63168829.
E-mail address: tytan@ntu.edu.sg (T.T.Y. Tan).

1010-6030/$ – see front matter © 2009 Elsevier B.V. All rights reserved.
doi:10.1016/j.jphotochem.2009.12.017

be enhanced by surface roughness [19,20]. Gan and co-workers reported that light induced superhydrophilicity of TiO_2 films were improved by controlling the roughness using polyethylene glycol [21]. Cebici and co-workers prepared nanoporosity-driven superhydrophilic thin films from layer-by-layer assembled silica and a polycation. They suggested that the superhydrophilicity is driven by the rapid infiltration of water into a 3D nanoporous network [22].

In the present work, we demonstrate the preparation of transparent C–N–F-codoped TiO_2 films via a simple dip-coating method without using additional pore-inducing agent. High transparency of the coating was achieved by a layer-by-layer coating method. A layer of TiO_2 was coated onto the glass substrate first before a second layer of NH_4F methanol solution was coated, followed by a third coating of TiO_2 sol. The first TiO_2 coating prevents the reactions of F^- ions with the glass substrate. Subsequent coatings of the NH_4F solution and the TiO_2 sol prevent immediate precipitation of the reactants. The ensuing heat treatment at 500 °C resulted in the reaction of NH_4F with the TiO_2 sol to form C–N–F-codoped TiO_2. The gaseous byproducts (NH_3 and HF) induced high surface roughness in the TiO_2 coated surface. Density functional theory (DFT) calculations were used to characterize the band gap of the codoped TiO_2 film. The reported method is promising in the preparation of visible-light active TiO_2-coated glass for self cleaning applications.

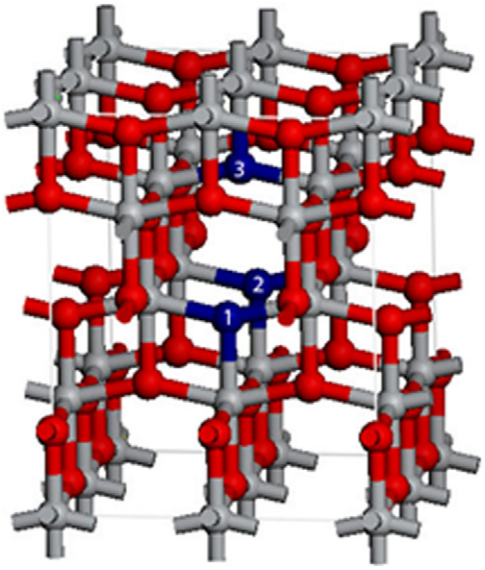

Fig. 1. $2 \times 2 \times 1$ supercell model of anatase TiO_2. Grey spheres—Ti atoms; red spheres—O atoms; blue spheres—doping sites. (For interpretation of the references to color in this figure legend, the reader is referred to the web version of the article.)

2. Experiments

2.1. Materials

Titanium (IV) isopropoxide (purity 97%), stearic acid (purity 95%), ammonium fluoride (purity 98%) and acetyl Acetone (purity 99%) were purchased from Sigma–Aldrich Co. Isopropanol and methanol was purchased from Merck.

2.2. Preparation of C–N–F-codoped TiO_2 film

TiO_2 sol was prepared using titanium (IV) isopropoxide as the Ti source. In a typical synthesis of TiO_2 sol, a mixture of 0.1 mL of distilled water and 10 mL of isopropanol was added drop-wise to the mixture of 2.5 g of TTIP and 10 mL of isopropanol. The solution was stirred in an oil bath at 80 °C for 18 h. 8 mL of acetylacetone (AcAc) was then added in the TiO_2 sol. Finally, the concentration of the TiO_2 sol was adjusted to 2.0 wt% by isopropanol.

Glass slides were used as coating substrates. Before deposition, the substrates were ultrasonically cleaned in distilled water, absolute ethanol, acetone and isopropanol for 15 min sequentially. TiO_2 thin films were deposited on the glass by a dip-coating process at room temperature. Firstly, one TiO_2 thin film was coated on the glass slides and calcined at 773 K for 1 h to prevent the reaction of NH_4F with glass. Then, the TiO_2 thin film was dipped in the NH_4F methanol solution (0.5, 1.0 and 2.0 wt%) and dried in vacuum at room temperature. Finally, one more TiO_2 layer was coated over the NH_4F layer and calcined at 773 K for 1 h. The obtained samples were marked as C–N–F-TiO_2-0.5, C–N–F-TiO_2-1 and C–N–F-TiO_2-2 for 0.5, 1.0 and 2.0 wt% NH_4F methanol solution, respectively. A C-TiO_2 film was prepared in a similar manner but without the NH_4F layer.

2.3. Characterization

X-ray diffraction analysis (XRD) was carried out by a Philips PW1010 X-ray diffractometer with Cu Kα radiation. XRD pattern was recorded with a scan step of 1° min^{-1} (2θ) in the range from 20° to 50°. X-ray photoelectron spectroscopy (XPS) analysis was carried out with a PHI Quantum 2000 Scanning ESCA Micro-probe equipment (Physical Electronics, MN, USA) using monochromatic Al-Kα radiation. The C–N–F-codoped TiO_2 film was etched by Ar ion to 10 nm to show the depth profile of C, N, F atoms in the TiO_2 lattice. The X-ray beam diameter was 100 μm, and the pass energy was 29.35 eV for the sample. The binding energy was calibrated with respect to C (1s) at 284.6 eV. Surface roughness and morphologies of C–N–F codoped TiO_2 film and TiO_2 film were evaluated by atomic force microscopy (AFM, MFP 3D). UV–vis spectra of films were obtained using a UV–visible spectrophotometer (Shimadzu). The sessile drop method was used for contact angle measurements with a FTA200 Dynamic Contact Angle analyzer. The contact angles were tested without light illumination and kept in dark for 1–30 days.

Photocatalytic degradation evaluation was performed using stearic acid as the model compound. The stearic acid layer was dispersed on the TiO_2 coated surface by spin coating (WS-400B-6NPPL/LITE). One 300 W halogen lamp held at 15 cm from the sample with a 420 nm UV filter was used as the visible light source. The change in stearic acid layer thickness was monitored by measuring the infrared absorption spectrum with a FTIR instrument (Digilab FTS 3100). The absorbance at 2917 cm^{-1}

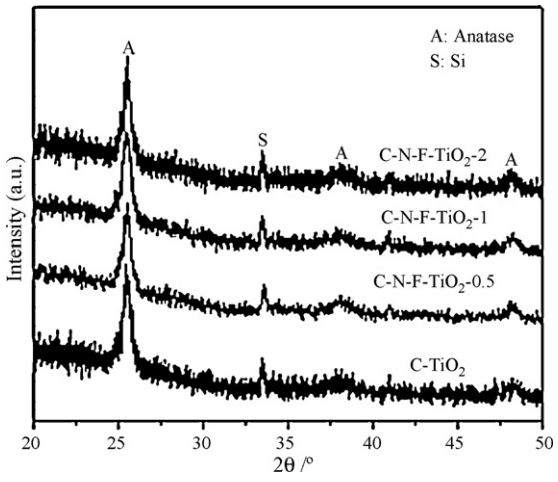

Fig. 2. XRD spectra of C–N–F-codoped TiO_2 and C-TiO_2 films.

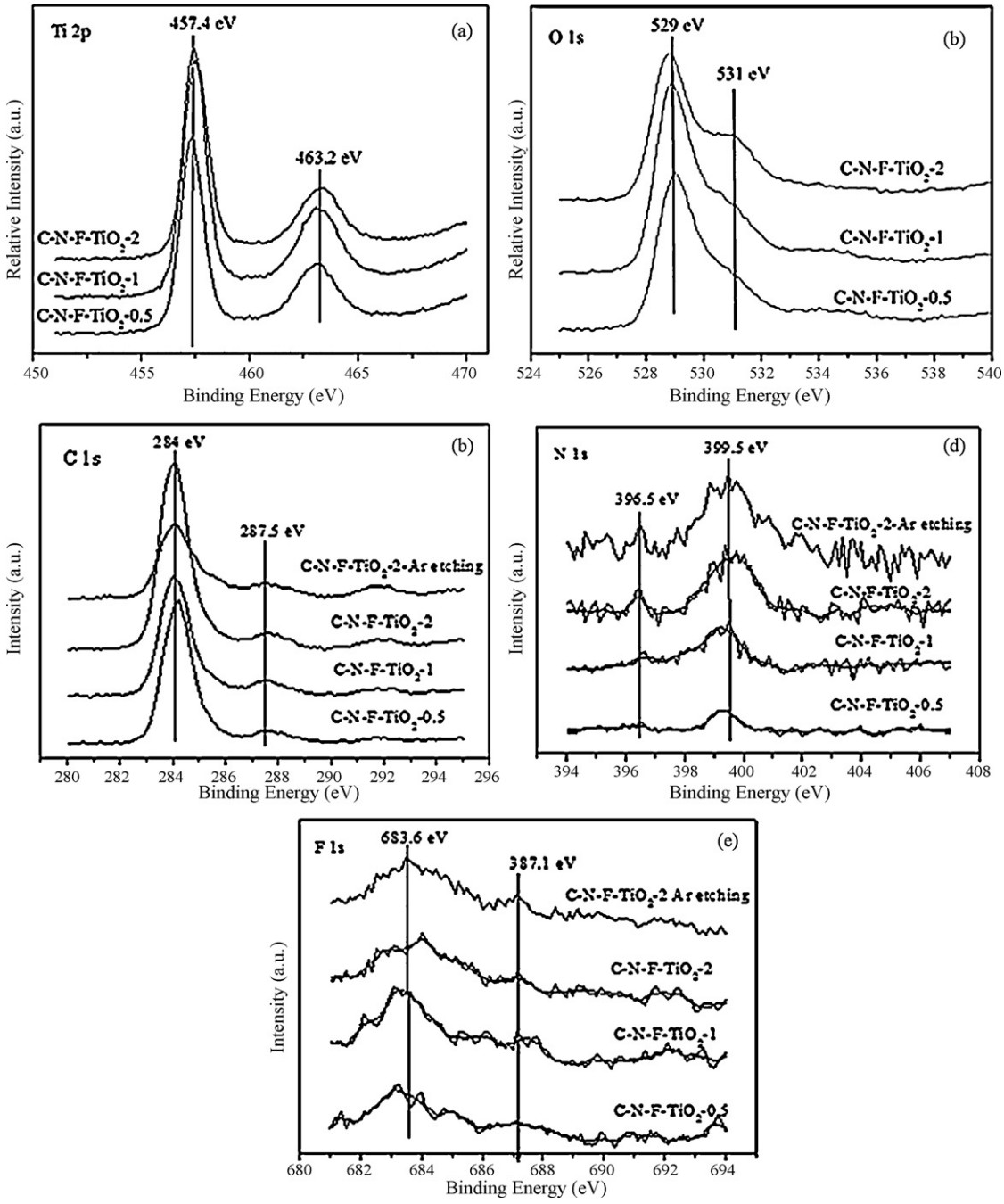

Fig. 3. (a) Ti 2p, (b) O 1s, (c) C 1s, (d) N 1s and (e) F 1s XPS spectra of C–N–F-codoped TiO_2 films, and (c) C 1s, (d) N 1s and (e) F 1s XPS spectra of C–N–F-TiO_2-2 film with Ar etching.

was converted to a thickness on the basis of an earlier observation that an absorbance of 0.01 corresponds to a thickness of 12.5 nm [5].

2.4. Theoretical calculations

Here, we calculated the band gap of TiO_2 and doped-TiO_2 using density functional theory (DFT) method. All the calculations were performed using generalized gradient approximation Perdew–Burke–Eznerhof (GGA–PBE) method [23] as implemented in Vienna *ab initio* simulation package [24]. $11 \times 11 \times 5$ Monkhorst–Pack grids [25] sampling and energy cutoff of 400 eV were used in our calculations. We used a $2 \times 2 \times 1$ supercell anatase TiO_2 crystal [26] containing 16 Ti atoms and 32 O atoms as our model. We doped TiO_2 by replacing the O atom(s) with N/F or both N and F atoms (see Fig. 1). Our optimized lattice constants of anatase TiO_2 are $a = b = 3.803$ and $c = 9.482$ Å which are in agreement with reported experimental value of $a = b = 3.785$ and $c = 9.514$ Å [26] and comparable to previously reported theoretical calculations of $a = b = 3.786$ and $c = 9.737$ Å [27], respectively.

3. Results and discussion

Fig. 2 shows the XRD patterns of C–N–F-TiO_2-0.5, C–N–F-TiO_2-1, C–N–F-TiO_2-2 and C-TiO_2 films. The distinctive peaks at $2\theta = 25.5^\circ$, 38.1° and 48.1° are attributed to the anatase crystal. The distinctive peak at $2\theta = 33.5^\circ$ is assigned to Si. There were no obvious peaks attributed to the rutile phase. From the XRD results we can infer

Table 1
Results of curve fitting of the XPS spectra for the Ti 2p, O 1s, C 1s, N 1s and F 1s regions.

Sample	Ti (at.%)	O (at.%)	C (at.%)	N (at.%)	F (at.%)	Roughness (nm)
C-TiO_2	15.2	47.9	36.9	0	0	1.0
C–N–F-TiO_2-0.5	13.4	44.2	41.9	0.2	0.3	2.9
C–N–F-TiO_2-1	14.0	47.7	37.3	0.6	0.4	5.8
C–N–F-TiO_2-2	11.3	44.9	42.6	0.8	0.4	10.0

that the C–N–F-TiO_2-0.5, C–N–F-TiO_2-1, C–N–F-TiO_2-2 and C-TiO_2 films mainly consist of anatase phase.

XPS was carried out to determine the chemical forms and concentrations of the C/N/F atoms in the C–N–F-TiO_2-0.5, C–N–F-TiO_2-1 and C–N–F-TiO_2-2 films. Fig. 3a–e shows the Ti 2p, O 1s, C 1s, N 1s and F 1s XPS spectra of the C–N–F-TiO_2-0.5, C–N–F-TiO_2-1 and C–N–F-TiO_2-2 films. In the spectra, the spin-orbit components ($2p_{3/2}$ and $2p_{1/2}$) of Ti 2p peaks at 457.4 eV and 463.2 eV indicate that Ti exists in the Ti^{4+} form. The O 1s spectrum shows a strong peak at 529 eV and a weak shoulder at around 531 eV, which are attributed to lattice oxygen of TiO_2 and surface hydroxides, respectively [28]. The C 1s spectrum shows a single strong peak at 284 eV and a weak shoulder at around 287.5 eV, which are attributed to elemental carbon and the carbonate species adsorbed on the surface, respectively [29]. Yang and co-workers reported a visible-light-active carbon and nitrogen co-doped TiO_2 catalyst using titanium isopropoxide as titanium and carbon sources [16]. Despite no Ti–C observed, the doped elemental carbon acted as a photo-sensitizer. The C–N-TiO_2 exhibited high activity under visible light and UV light and it was suggested that the dopants enhanced the separation of photoexcited electrons and holes [16]. For the N 1s spectrum, a large peak appeared at 399.5 eV and a small peak appeared at 396.5 eV. The large peak is assigned to the N atoms from adsorbed N-containing compounds, while the 396.5 eV peak is generally considered as evidence for the presence of Ti–N bonds in the TiO_2 crystal lattice [2]. For the F 1s XPS spectra, the peak located at 687.8 eV is attributed to the substitutional F atoms in TiO_2 crystal lattice, and the large peak located at around 684.5 eV is originated from the F-containing compounds [4,30]. In order to show the depth profile of C, N, F atoms incorporated into the lattice of TiO_2, XPS with Ar etching was performed (Fig. 3c–e). It was found that the XPS spectra of N and F with Ar etching were similar to that of the spectra without Ar etching. This suggested that the N and F atoms were also incorporated into the TiO_2 lattice. For the carbon spectrum, it was found that carbon also existed as elemental carbon and carbonate species. However, the concentration of carbon in the C–N–F-TiO_2-2 film decreased to 18.2 at.%, which could be attributed to the elimination of organic contamination on the surface of C–N–F-TiO_2-2 film by Ar etching.

Based on the XPS results, the total Ti, O, C, N and F concentrations are shown in Table 1. The concentrations of N and F in the C–N–F-codoped TiO_2 are 0.2–0.8 at.% and 0.3–0.4 at.%, respectively. Valentin and co-workers reported that NH_4F can react with TiO_2 gel to form N–F-codoped TiO_2 at 770 K [17]. Therefore, it is not surprising to find N and F doped in TiO_2 prepared by the current method, despite their low concentrations. A low N concentration has been shown to improve photocatalytic activities of TiO_2 under visible light [31].

The UV–visible diffuse reflectance spectra of the transparent C–N–F-TiO_2-0.5, C–N–F-TiO_2-1, C–N–F-TiO_2-2 and C-TiO_2 films are shown in Fig. 4. For the C–N–F-codoped TiO_2 films, the absorption edges are extended to the visible light region, which are away from the absorption edge of C-TiO_2 film. For the C dopant in the TiO_2 films, elemental C is incorporated in the TiO_2 matrix interstitially and carbonate species are adsorbed on the surface (as determined from XPS). They have no effect on TiO_2 band gap narrowing and are believed to act as a photosensitizer. It was reported that doping of F atoms alone also did not cause significant red shift of

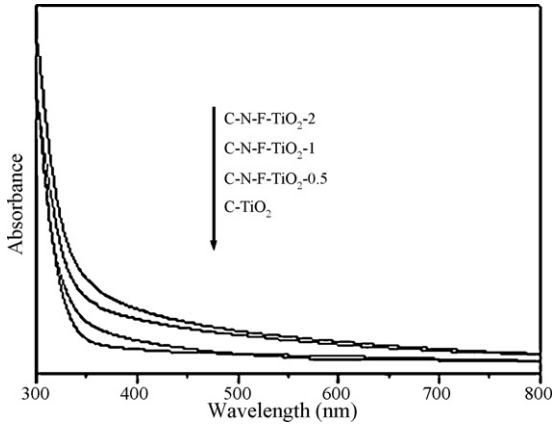

Fig. 4. UV–visible diffuse reflectance spectra of C–N–F-codoped TiO_2 and C-TiO_2 films.

the TiO_2 absorption edge [30]. Asahi et al. reported that N doping could shift the absorption edge to visible light due to the band-gap narrowing of TiO_2 [2]. Other groups reported that the red shift of nitrogen doped TiO_2 was due to the formation of isolated levels [32,33]. Therefore, the red shift was mainly attributed to the nitrogen doping in C–N–F-codoped TiO_2 films [16]. The synergy of the C/N/F dopants in the C–N–F-codoped TiO_2 films could result in more photogenerated electrons and holes for improved visible light photocatalytic reactions [30]. This will be further discussed in the following paragraphs.

Using DFT calculation, the calculated band gap differences, ΔE_{gap}, between TiO_2 and doped TiO_2 are listed in Table 2. Our results show that the F doping has negligible effects on band gap of anatase TiO_2 with $\Delta E_{gap} = 0.06$ eV, consistent with another report that doping of F atoms did not cause significant red shift of the TiO_2 absorption edge [30]. In contrast, N-doping decreases the band gap of TiO_2 with $\Delta E_{gap} = -0.35$ and -0.54 eV for N-TiO_2 and 2N-TiO_2, respectively, consistent with report of N doping lead to band-gap narrowing of TiO_2 [2]. This effect is prevalent even for N–F co-doped

Table 2
Band gap differences, ΔE_{gap} (in eV), of N/F-doped TiO_2. Pure TiO_2 is taken as the reference band gap. Refer to Fig. 1 for definition of doping sites.

Systems	ΔE_{gap}
N-TiO_2[a]	−0.35
2N-TiO_2[b]	−0.54
F-TiO_2[a]	0.06
2F-TiO_2[b]	0.06
N, F-TiO_2[c]	−0.38
2N, F-TiO_2[d]	−0.48
N, 2F-TiO_2[e]	−0.26

[a] O1 is replaced by either N or F.
[b] O1 and O2 both are replaced by either N or F atoms.
[c] O1 and O2 are replaced by N and F atoms.
[d] O1 and O2 are replaced by N atoms and O3 is replaced by F atom.
[e] O1 is replaced by N atom, and O2 and O3 are replaced by F atoms.

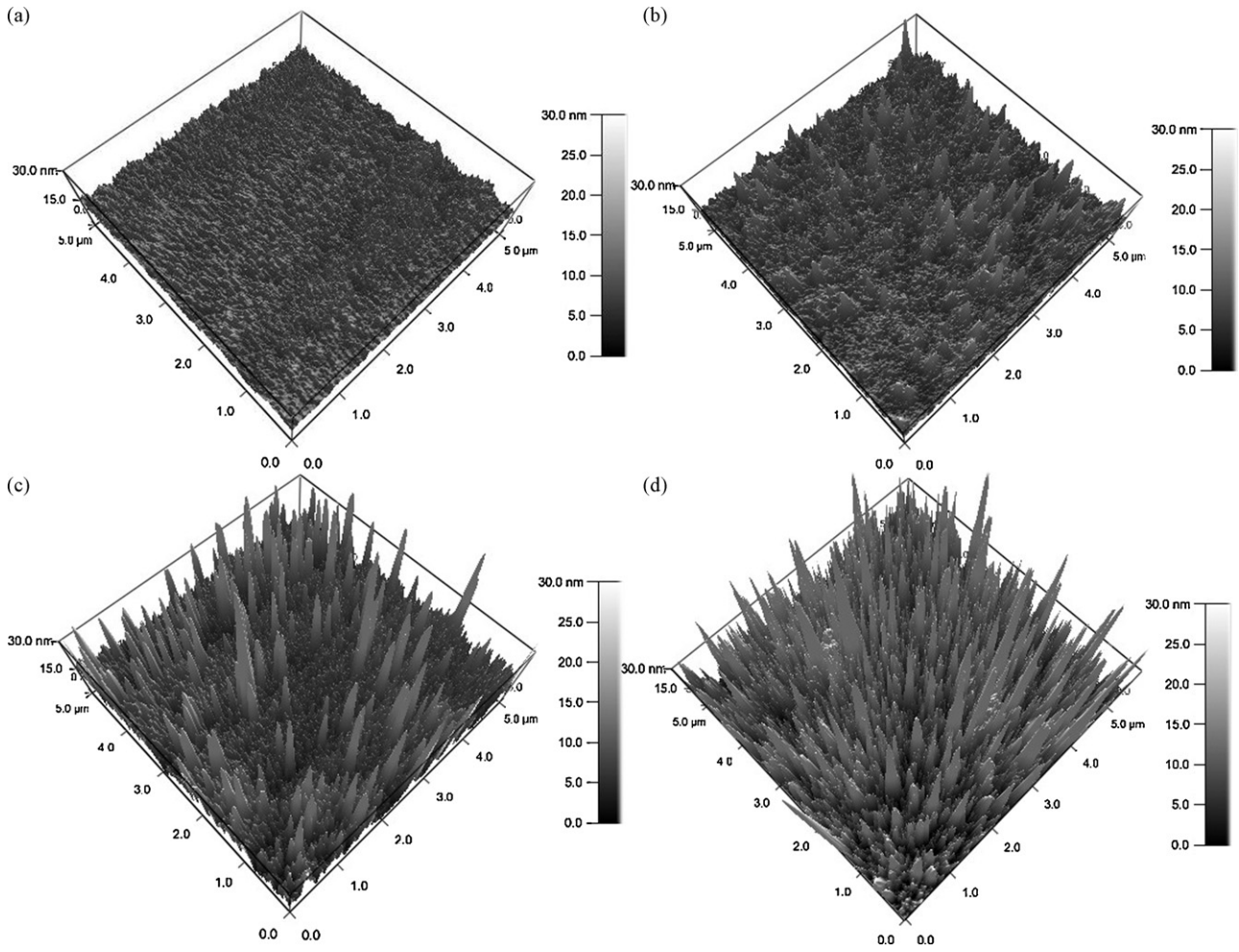

Fig. 5. AFM 3D images of the surface of (a) C-TiO_2 film; (b) C–N–F-TiO_2-0.5 film; (c) C–N–F-TiO_2-1 film; (d) C–N–F-TiO_2-2 film.

TiO_2 with $E_{gap} = -0.38$, -0.48 and -0.26 eV for N, F-TiO_2, 2N, F-TiO_2, and N, 2F-TiO_2, respectively. Here, we observed that band gap decreased with increased N:F doping ratio which is consistent with the current experimental observation of red shift in the absorbance curves (see Fig. 4) with increase N:F doping ratio. We did not include C doping in the calculation as it acts as a photosensitizer and therefore has no effect on the TiO_2 band gap.

Fig. 5 shows the AFM 3D images of the surface of C-TiO_2, C–N–F-TiO_2-0.5, C–N–F-TiO_2-1 and C–N–F-TiO_2-2 films. The C-TiO_2 film (Fig. 5a) has a relatively flat structure with low surface roughness (1.0 nm). However, it is obvious from the AFM 3D images (Fig. 5b–d) that the surface roughness of the C–N–F-codoped TiO_2 films increase with the increasing NH_4F concentration. Their surface roughness is much higher than that of C-TiO_2 film. The surface roughnesses of C–N–F-TiO_2-0.5, C–N–F-TiO_2-1 and C–N–F-TiO_2-2 films are 2.9 nm, 5.8 nm and 10.0 nm, respectively (Table 1). NH_3 and HF were formed from the decomposition of NH_4F at the calcination temperature. These gaseous byproducts evolved within the TiO_2 film, generating pores in the process and therefore inducing surface roughness in the TiO_2 film. With the increase of NH_4F concentration, the amount of gaseous byproducts (NH_3 and HF) is expected to increase, which lead to the increase of surface roughness.

It is well known that the contact angle of TiO_2 film decreases gradually to almost zero when it is irradiated by UV light. Yu and co-workers reported that a typical non-porous TiO_2 thin film cannot maintain this hydrophilic state in the dark [20]. As soon as the thin film is placed in the dark, the water contact angle increases. From a practical point of view for self-cleaning surfaces, it is desirable that the contact angle remain <5° for a long time without the need of illumination. The stability of hydrophilic properties can be enhanced by surface roughness. Contact angle measurement have been undertaken to study the superhydrophilicity of C–N–F codoped TiO_2 films and C-TiO_2 film. The contact angles of the C-TiO_2, C–N–F-TiO_2-0.5, C–N–F-TiO_2-1 and C–N–F-TiO_2-2 films are 4.6°, 3.1°, 2.6° and 2.3°, respectively, after being kept in the dark for 24 h and without any illumination. Fig. 6a shows the contact angles of C-TiO_2, C–N–F-TiO_2-0.5, C–N–F-TiO_2-1 and C–N–F-TiO_2-2 films which had been being kept in the dark for different duration. The contact angels of C–N–F-TiO_2-1 and C–N–F-TiO_2-2 films remain relatively low at 4.1° and 3.1°, respectively, even after being kept in the dark for 30 days. However, the contact angles of C-TiO_2 increase to 19.2°. The "long-term" superhydrophilicity of the C–N–F-TiO_2-1 and C–N–F-TiO_2-2 is beneficial for self-cleaning application. The superhydrophilicity of C–N–F-codoped TiO_2 films is mainly due to the high roughness and highly accessible pores in the C–N–F-codoped TiO_2 films that reduce diffusion-resistance within the film structure, and subsequently allows a better penetration of water through the void [21].

To the best of our knowledge, there is no report in open literature about F-doped TiO_2 films coated on glass slides for self-cleaning application. This is probably because HF and NH_4F can react with glass slide, which lead to the corrosion of the glass and render it non-transparent. In this work, we coated a crystalline TiO_2 film on the glass slide first to prevent NH_4F and HF from reacting with the glass. Fig. 6b shows the image of glass slide coated with C–N–F-

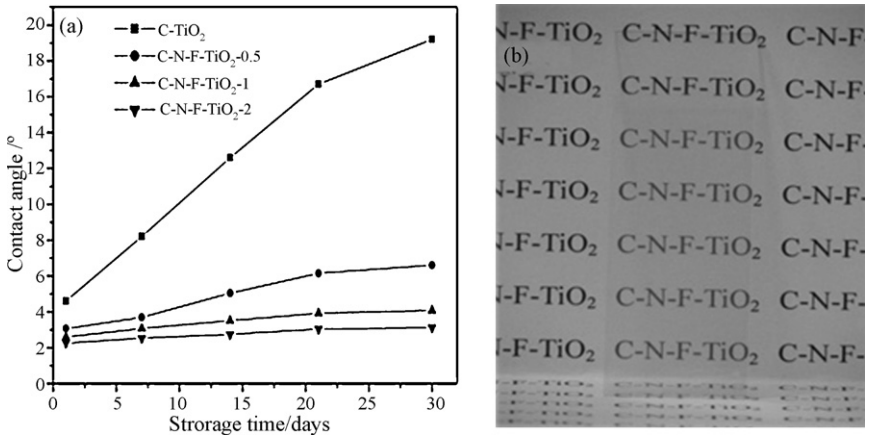

Fig. 6. (a) Contact angles of C–N–F-codoped TiO_2 and C-TiO_2 films kept in the dark for different days, and (b) picture of C–N–F-TiO_2-1 glass.

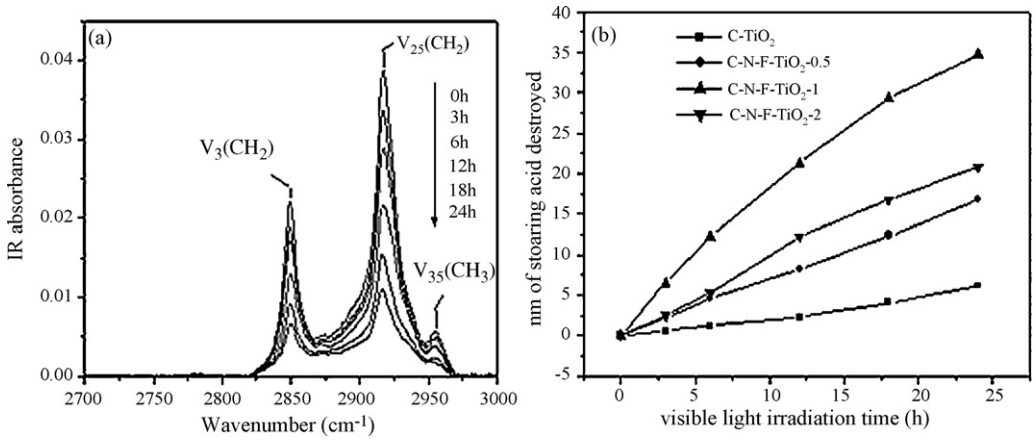

Fig. 7. (a) Evolution of the IR absorbance spectra (C–N–F-TiO_2-1 film) for different illumination times under visible light. Decrease in stearic acid layer thickness for different illumination times under and (b) visible light.

TiO_2-1 film. It is transparent and shows a yellow tint due to the doping of C, N and F in the TiO_2.

The photocatalytic activity of C–N–F-codoped TiO_2 and C-TiO_2 films were evaluated by monitoring the degradation of stearic acid under visible light. IR absorbance spectra of stearic acid obtained under different illumination times are displayed (Fig. 7a), showing the disappearance of stearic acid absorbance at different time. The absorbance is then converted to thickness of stearic acid disappearance (in nm). Fig. 7b shows that the photocatalytic activities of C–N–F-codoped TiO_2 films under visible light are much higher than that of C-TiO_2 film. The kinetics of stearic acid destruction appears to be zero-order initially with respect to the thickness of stearic acid decomposed. This result is consistent with the result reported by Pore and co-workers [5]. Optimum dopant concentration was encountered for C–N–F-codoped TiO_2 (C–N–F-TiO_2-1) film, which degrades stearic acid at a rate of 1.57 nm h^{-1}, more than 5 times higher than that of C-TiO_2 film (0.24 nm h^{-1}). For the C–N–F-codoped TiO_2 films, it is suggested that the enhanced photocatalytic activities under visible light are mainly attributed to the synergetic effect between doped N, F and C atoms, and the high surface area induced. It has been reported that the doped carbon acted as a photosensitizer, which could be excited to inject electrons into the conduction bands of TiO_2 [16]. The electrons could then be transferred to the surface-adsorbed oxygen molecules and form superoxide anions, which could further transform to $OH^{\bullet}$ and initiate the degradation of stearic acid [16]. The doped N atoms improve the visible light absorption, while the doped F atoms can facilitate the formation of oxygen vacancies, which are generally regarded as an important active species for initiating a photocatalytic reaction [30]. Moreover, high surface area can improve adsorption of stearic acid onto the TiO_2 surface, improving the photodegradation efficiency [34]. It can also be seen that the photocatalytic activity of C–N–F-TiO_2-2 is lower than that of C–N–F-TiO_2-1. This is ascribable to the greater number of doping sites at higher dopant concentration, which could serve as charge recombination sites. Therefore, beyond an optimal dopant concentration, higher dopant concentration may lead to a higher charge recombination rate and a lower the photocatalytic activity [32].

4. Conclusion

Transparent C–N–F-codoped TiO_2 films were coated on glass substrates by a simple layer-by-layer dip-coating method. The surface roughness of the C–N–F-codoped TiO_2, achieved without the need of an additional pore-inducing agent, was higher than that of C-TiO_2 film. The high surface roughness hindered the conversion of the C–N–F-codoped TiO_2 films from a hydrophilic to a hydrophobic state in the dark and led to the superhydrophilicity without any illumination for up to 30 days. The C–N–F-codoped TiO_2 films showed higher visible-light photocatalytic activities for stearic acid decomposition compared to that of C-TiO_2 film. This is attributed to a synergetic effect of the doped C, N and F atoms, and a higher surface area. Our DFT calculations also showed that an increased N:F doping ratio leads to band gap narrowing of TiO_2, consistent with the cur-

rent experimental observation of red shift in the absorbance curve with increasing N:F doping ratio. The current simple approach of coating doped TiO_2 nanoparticles onto glass substrates could potentially be applied to other substrates for the preparation of transparent and superhydrophilic doped TiO_2 surface coating for self-cleaning and other applications.

Acknowledgements

Financial support from Nanyang Technological University AcRF Tier 1 RG29/07 is gratefully acknowledged. D.V.W. and M.A.S. are grateful for their scholarships awarded by NTU.

References

[1] R. Wang, K. Hashimoto, A. Fujishima, M. Chikuni, E. Kojima, A. Kitamura, M. Shimohigoshi, T. Watanabe, Light-induced amphiphilic surfaces, Nature 338 (1997) 431–432.
[2] R. Asahi, T. Morikawa, T. Ohwaki, K. Aoki, Y. Taga, Visible-light photocatalysis in nitrogen-doped titanium oxides, Science 293 (2001) 269–271.
[3] S.U.M. Khan, M. Al-Shahry, W.B. Ingler, Efficient photochemical water splitting by a chemically modified n-TiO_2, Science 297 (2002) 2243–2245.
[4] J.C. Yu, J. Yu, W. Ho, Z. Jiang, L. Zhang, Effects of F^- doping on the photocatalytic activity and microstructures of nanocrystalline TiO_2 powders, Chem. Mater. 14 (2002) 3808–3816.
[5] V. Pore, M. Ritala, M. Leskela, S. Areva, M. Jarn, J. Jarnstrom, H_2S modified atomic layer deposition process for photocatalytic TiO_2 thin films, J. Mater. Chem. 17 (2007) 1361–1371.
[6] D. Dvoranova, V. Brezova, M. Mazur, M.A. Malati, Investigations of metal-doped titanium dioxide photocatalysts, Appl. Catal. B-Environ. 37 (2002) 91–105.
[7] S.T. Martin, C.L. Morrison, M.R. Hoffmann, Photochemical mechanism of size-quantized vanadium-doped TiO_2 particles, J. Phys. Chem. 98 (1994) 13695–13704.
[8] X.Y. Li, P.L. Yue, C. Kutal, Synthesis and photocatalytic oxidation properties of iron doped titanium dioxide nanosemiconductor particles, New J. Chem. 27 (2003) 1264–1269.
[9] A. Borras, C. Lopez, V. Rico, F. Gracia, A.R. Gonzalez-Elipe, E. Richter, G. Battiston, R. Gerbasi, N. McSporran, G. Sauthier, E. Gyorgy, A. Figueras, Effect of visible and UV illumination on the water contact angle of TiO_2 thin films with incorporated nitrogen, J. Phys. Chem. C 111 (2007) 1801–1808.
[10] M. Miyauchi, Visible light induced super-hydrophilicity on single crystalline TiO_2 nanoparticles and WO_3 layered thin films, J. Mater. Chem. 18 (2008) 1858–1864.
[11] H. Irie, S. Washizuka, N. Yoshino, K. Hashimoto, Visible-light induced hydrophilicity on nitrogen-substituted titanium dioxide films, Chem. Commun. (2003) 1298–1299.
[12] T. Tachikawa, Y. Takai, S. Tojo, M. Fujitsuka, H. Irie, K. Hashimoto, T. Majima, Visible light-induced degradation of ethylene glycol on nitrogen-doped TiO_2 powders, J. Phys. Chem. B 110 (2006) 13158–13165.
[13] J.H. Xu, J. Li, W.L. Dai, Y. Cao, H. Li, K. Fan, Simple fabrication of twist-like helix N,S-codoped titania photocatalyst with visible-light response, Appl. Catal. B: Environ. 79 (2008) 72–80.
[14] D. Li, H. Haneda, S. Hishita, N. Ohashi, Visible-light-driven N–F-codoped TiO_2 photocatalysts. 1. Synthesis by spray pyrolysis and surface characterization, Chem. Mater. 17 (2005) 2588–2595.
[15] G. Liu, Y. Zhao, C. Sun, F. Li, G.Q. Lu, H.M. Cheng, Synergistic effects of B/N doping on the visible-light photocatalytic activity of mesoporous TiO_2, Angew. Chem. Int. Ed. 47 (2008) 4516–14516.
[16] X. Yang, C. Cao, L. Erickson, K. Hohn, R. Maghirang, K. Klabunde, Synthesis of visible-light-active TiO_2-based photocatalysts by carbon and nitrogen doping, J. Catal. 260 (2008) 128–133.
[17] C. Di Valentin, E. Finazzi, G. Pacchioni, Density functional theory and electron paramagnetic resonance study on the effect of N–F codoping of TiO_2, Chem. Mater. 20 (2008) 3706–3714.
[18] T. Lindgren, J.M. Mwabora, E. Avendano, J. Jonsson, A. Hoel, C.G. Granqvist, S.E. Lindquist, Photoelectrochemical and optical properties of nitrogen doped titanium dioxide films prepared by reactive DC magnetron sputtering, J. Phys. Chem. B 107 (2003) 5709–5716.
[19] Charlene J.W. Ng, H. Gao, Timothy T.Y. Tan, Atomic layer deposition of TiO_2 nanostructures for self-cleaning applications, Nanotechnology 19 (2008) 445–604.
[20] J.C. Yu, J. Yu, H.Y. Tang, L. Zhang, Effect of surface microstructure on the photoinduced hydrophilicity of porous TiO_2 thin films, J. Mater. Chem. 12 (2002) 81–85.
[21] W.Y. Gan, S.W. Lam, K. Chiang, R. Amal, H. Zhao, M.P. Brungs, Novel TiO_2 thin film with non-UV activated superwetting and antifogging behaviours, J. Mater. Chem. 17 (2007) 952–954.
[22] F.C. Cebeci, Z. Wu, L. Zhai, R.E. Cohen, M.F. Rubner, Nanoporosity-driven superhydrophilicity: a means to create multifunctional antifogging coatings, Langmuir 22 (2006) 2856–2862.
[23] J.P. Perdew, K. Burke, M. Ernzerhof, Generalized gradient approximation made simple, Phys. Rev. Lett. 77 (1997) 3865–3868.
[24] G. Kresse, J. Furthmuller, Efficient iterative schemes for ab initio total-energy calculations using a plane-wave basis set, Phys. Rev. B 54 (1996) 11169–11186.
[25] H.J. Monkhorst, J.D. Pack, Special points for brillouin-zone integrations, Phys. Rev. B 13 (1976) 5188–5192.
[26] D.T. Cromer, K. Herrington, The structures of anatase and rutile, J. Am. Chem. Soc. 77 (1955) 4708–4709.
[27] M. Lazzeri, A. Vittadini, A. Selloni, Structure and energetics of stoichiometric TiO_2 anatase surfaces, Phys. Rev. B 63 (2001) 155409.
[28] C.L. Yu, J.C. Yu, A simple way to prepare C–N-codoped TiO_2 photocatalyst with visible-light activity, Catal. Lett. 129 (2009) 462–470.
[29] X. Wang, S. Meng, X. Zhang, H. Wang, W. Zhong, Q. Du, Multi-type carbon doping of TiO_2 photocatalyst, Chem. Phys. Lett. 444 (2007) 292–296.
[30] D.G. Huang, S.J. Liao, J.M. Liu, Z. Dang, L. Petrik, Preparation of visible-light responsive N–F-codoped TiO_2 photocatalyst by a sol–gel-solvothermal method, J. Photochem. Photobiol. A 184 (2006) 282–288.
[31] H. Sun, Y. Bai, W. Jin, N. Xu, Visible-light-driven TiO_2 catalysts doped with low-concentration nitrogen species, Sol. Energy Mater. Sol. Cells 92 (2008) 76–83.
[32] H. Irie, Y. Watanabe, K. Hashimoto, Nitrogen-concentration dependence on photocatalytic activity of $TiO_{2-x}N_x$ powders, J. Phys. Chem. B 107 (2003) 5483–5486.
[33] R. Nakamura, T. Tanaka, Y. Nakato, Mechanism for visible light responses in anodic photocurrents at N-doped TiO_2 film electrodes, J. Phys. Chem. B 108 (2004) 10617–10620.
[34] E. Allain, S. Besson, C. Durand, M. Moreau, T. Gacoin, J.P. Boilot, Transparent mesoporous nanocomposite films for self-cleaning applications, Adv. Funct. Mater. 17 (2007) 549–554.